Carbon partitioning and structure evolution in the hardening treatments of high strength steel

LUO, Quanshun <http://orcid.org/0000-0003-4102-2129>, KITCHEN, Matthew, PATEL, Vinay and MAGOWAN, Stephen

Published version

LUO, Quanshun, KITCHEN, Matthew, PATEL, Vinay and MAGOWAN, Stephen (2012). Carbon partitioning and structure evolution in the hardening treatments of high strength steel. In: 20th Congress of International Federation for Heat Treatment and Surface Engineering, Beijing, China, 23-25 October 2012. (Unpublished)

Carbon partitioning and structure evolution in the hardening treatments of high strength steel

Quanshun Luo, Matthew Kitchen, Vinay Patel, Stephen Magowan

Materials and Engineering Research Institute, Sheffield Hallam University, Howard Street, Sheffield, S1 1WB, UK

Abstract: In this paper, we report the microstructural evolution and carbon partitioning behaviour of an alloyed medium carbon steel in continuous quenching and the subsequent tempering process. The obtained samples were characterized by XRD with Gaussian peak-fitting analysis, field-emission-gun SEM, and TEM. It has been found that, the oil quenched sample was hardened to HV 742, exhibiting a mixed microstructure of plate- and lath-type martensites with a 8.0% volume fraction of retained austenite, as well as a small number of un-dissolved carbide particles. Carbon partitioning was evidenced in the as-quenched structure by supersaturation of carbon to 0.93 wt% in the retained austenite. Moreover, careful peak-fitting analysis of the martensite diffraction peak $\{200\}_M$ suggested the existence of two martensitic structures having different carbon contents, namely 0.41% and 0.19 wt% respectively, which corresponded to the lath- and plate-type martensites as verified by TEM observation. Slower cooling rates in thick samples have been found to facilitate more pronounced carbon partitioning, which included the diffusion of carbon from the newly formed martensite to the un-transformed austenite and the precipitation of carbide particles in the martensite/ferrite matrix. Subsequent tempering following the quenching treatment resulted in a decrease in hardness from 677HV to 542HV due to the recovery of lattice strains in the martensite and, when tempered at 300^0C or higher temperatures, significant decrease in carbon contents with martensite.

Key Words: Carbon partitioning; Heat treatments; Steel; X-ray diffraction; Gaussian peak-fitting

CARBON PARTITIONING refers to the diffusion of carbon atoms from super-saturated martensite and or bainite to under-cooled austenite in the hardening heat treatments of steels. In recent years, several novel heat treatment processes have emerged in developing carbide-free bainitic steels[1-5] and duplex martensite and austenite steels[6-9]. These technological advances are attracting comprehensive studies about microstructural evolution during the transformation of under-cooled austenite to bainite or martensite, especially the phenomenon of carbon partitioning. In fact, carbon partitioning in martensite transformation was addressed in literature long time ago[10-14]. Carbon as an essential chemical component provides the most important basis for various strengthening mechanisms of steels. It also has significant influence on the transformation temperature of under-cooled austenite. Several recently published articles have reported carbon partitioning in isothermal treated bainitic steels[3, 15-16], in partially quenched and partitioning treated martensitic steels[7, 14, 17-18] and in a tempered bainitic steel[19].

Quantitative study of carbon partitioning depends strictly on accurate measurement of carbon contents in various matrix phases. X-ray diffraction is well known for its high precision in quantitative crystallography measurements. The principle is based on the linear relationships between the carbon content and the lattice parameter of austenite[20] and or the tetragonal ratio (i.e. the c/a ratio) of martensite[21]. The measurements, however, are practically not easy in the case of hardened steels, either because of the very small volume fractions of retained austenite or due to the extremely strong lattice distortion of martensite which leads to significant broadening of the diffraction peaks. Alternative techniques of carbon content measurements have been reported to include the dilatometric method[15, 22], transmission electron energy loss spectroscopy (EELS), and atom probe topography (APT)[14, 16-19]. The dilatometric method is in principle based on the measurement of the Ms temperature, namely, the starting temperature of austenite-to-martensite transformation. But it fails to distinguish the carbon contents of newly formed martensite and the retained austenite. EELS is a powerful analytical tool both in detecting light elements and in characterizing the chemical bonding of compounds[23,24], whereas there might be technical problems regarding preparation of ultra-clean samples free from surface contamination. APT is a newly emerging analytical tool providing carbon content measurement at extremely high spatial resolution, e.g. in nano-scales across the austenite to martensite and or austenite to bainite interfaces[2, 19]. In particular, some papers reported good consistency in carbon contents measured by XRD and APT methods[3, 15, 16].

In this paper, we present the carbon partitioning behaviour of a medium carbon steel in continuous cooling as well as in subsequent tempering treatments. The effect of cooling conditions on the carbon partitioning behaviour is reported. Along with microstructural characterization by means of

scanning electron microscopy (SEM) and transmission electron microscopy (TEM), comprehensive analyses were carried out using quantitative XRD measurements assisted with multiple Gaussian peak-fitting.

1. Experimental

1.1 Material, heat treatments and sample preparation

Experimental samples were taken from hot rolled alloy steel having chemical compositions modified from AISI L6 (in wt%: C 0.5-0.6, Si+Mn 0.8-1.3, Cr 0.6-1.2, Ni 1.2-2.0, Mo+V 0.6-0.8, Fe in balance). Two types of samples were prepared, namely blocks of 8×10×20 mm in size for standard hardening and tempering treatments and cylindrical bars of 50 mm in diameter and 60 mm in length for hardening at slower cooling conditions. The heat treatments were carried out using a digitally programmed electrical resistance, muffle furnace. Table 1 lists the conducted heat treatments.

Before hardness testing and subsequent analyses, the as-treated surfaces were ground using 120# or 240# abrasive papers to remove the softened layer by at least 0.4 mm. For the cylindrical samples, an 8 mm thick slice was taken from the middle length by cutting the cylindrical section using wire spark erosion technique under cooling, to minimize sample heating. Vickers' hardness tests were carried out on ground sample surfaces being ground using 320# SiC abrasive papers. The applied indentation load was 30kg. An average value was made from five indents.

The samples for XRD and SEM observations were ground and polished following the standard metallographic preparation procedure and finished with careful polishing using a 1μm diamond slurry. SEM samples were etched using a 2% nital solution. The samples for TEM observations were first ground to a thin foil approximately 120-150 microns thick, and then finished by electro-chemical polishing using a TenuPol-5 twinjet electropolishing device using a electrolyte composed of 7% perchloric acid and 93% glacial acetic acid at room temperature and a voltage of 32 V.

1.2 Characterization

A high resolution instrument, FEI NOVA200 FEG-SEM, was employed for the microstructural observation. A Philips CM20 TEM was used to characterize the martensite sub-structures on selected samples. The instrument has a W-filament and was operated at 200 kV.

Quantitative XRD analysis was used to determine the fraction and lattice parameter of retained austenite and the tetragonal ratio of martensite. X-ray diffraction measurements were performed by employing a Philips X'Pert X-ray diffractometer using a Cu X-ray emitter at 40kV and 40 mA. XRD data of five diffractions, namely the austenite peaks $\{200\}_\gamma$, $\{220\}_\gamma$ and $\{311\}_\gamma$, and the martensite peaks $\{200\}_\alpha$ and $\{211\}_\alpha$, were collected at the Bragg-Brentano mode using a step size 0.03^0 and a long acquisition time of 1,000 seconds per step. An example of the acquired diffractions is shown in Figure 1.

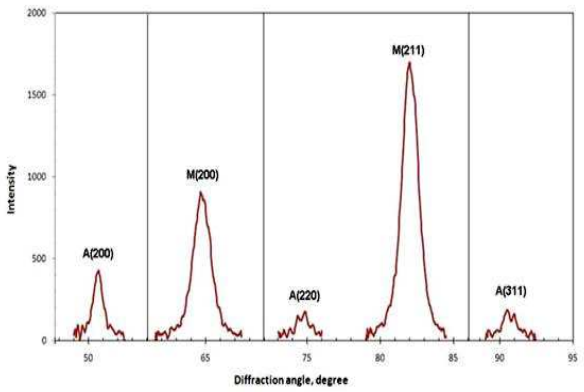

Fig. 1 XRD peaks of the oil-quenched sample: namely {200}, {220} and {311} of austenite and {200} and {211} of martensite.

The volume fraction of retained austenite (A%) was calculated using equation $A\% = I_A / (I_A + G \cdot I_M)$, where I_A and I_M stand for the integrated intensities of the austenite and martensite diffraction peaks respectively and G is a constant depending on the combination of the austenite and martensite planes.

Table 1 Heat treatments and resulting hardness of the samples.

No.	Samples	Austenisation	Cooling	Tempering	HV_{30}
1	8 mm block	850^0C / 25 min	Oil	n/a	742±9
2	8 mm block	850^0C / 25 min	Oil	200^0C / 120 min	677±17
3	8 mm block	850^0C / 25 min	Oil	300^0C /120 min	588±14
4	8 mm block	850^0C / 25 min	Oil	400^0C / 120 min	542±4
5	5 mm depth of cylinder	850^0C / 30 min	Oil	n/a	717±3
6	Core of cylinder	850^0C / 30 min	Oil	n/a	704±11
7	5 mm depth of cylinder	850^0C / 30 min	Air	n/a	464±13
8	Core of cylinder	850^0C / 30 min	Air	n/a	422±16

The values of the *G* constants were adopted from selected literature [20, 21, 25].

To determine the carbon content of retained austenite, a self-developed Gaussian peak-fitting technique was employed to determine the 2θ values of the small and broad $\{200\}_\gamma$, $\{220\}_\gamma$ and $\{311\}_\gamma$ diffractions [26, 27]. Then the austenite lattice parameter was calculated by averaging the three values obtained from the d-spacings. Consequently the carbon content of the retained austenite, C% in weight percent, was estimated using the formula suggested by Abbaschian et al [20]: $a_0 = 0.3555 + 0.0044 \cdot C\%$.

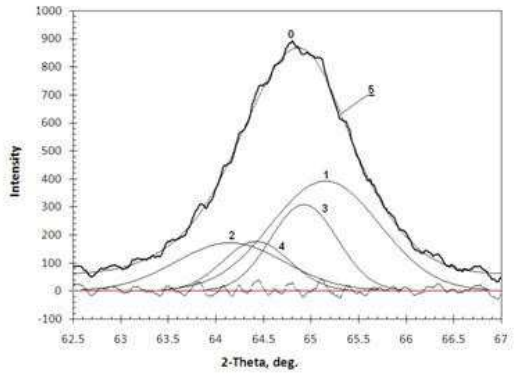

Fig. 2 Multiple Gaussian peak-fitting of the $\{200\}_M$ peak of the oil-quenched sample martensite: (0) original diffraction; (1&2) diffractions of plate-type martensite; (3&4) diffractions of lath-type martensite; and (5) sum of peaks 1-4.

The carbon content of martensite was determined from the XRD data according to the linear relationship of carbon content to the tetragonal ratio (c/a): $C\% = [0.28661 \times (c/a - 1)]/[0.00124 + 0.0115 \times c/a]$ [20,21]. Gaussian peak-fitting was applied to deconvolute the $\{200\}_M$ diffraction peak to two sub-peaks of $(200)/(020)_M$, and $(002)_M$ in order to determine the tetragonal ratio. However, it was found that the $\{200\}_M$ peaks collected on the investigated samples did not fit well to a two-peak model. This phenomenon was believed to be attributed to the mixed martensite substructures. Therefore, the lath-like martensite should have a different carbon content and thereby a different c/a ratio from the plate-like martensite as suggested in the literature[11, 28]. Consequently, a multiple four-peak Gaussian fitting programme was developed to determine the c/a ratios and volume fractions of the two types of martensites. An example of the four-peak fitting is shown in Figure 2.

To the knowledge of the authors, such quantitative separation of martensite sub-structures is reported for the first time.

2. Results and discussion

2.1 Microstructure and carbon partitioning in as-quenched steel

Figure 3 is a back-scattered SEM image showing the microstructure of the as-quenched steel. The microstructure is a mixture of martensitic laths and plates as well as a small amount of retained austenite.

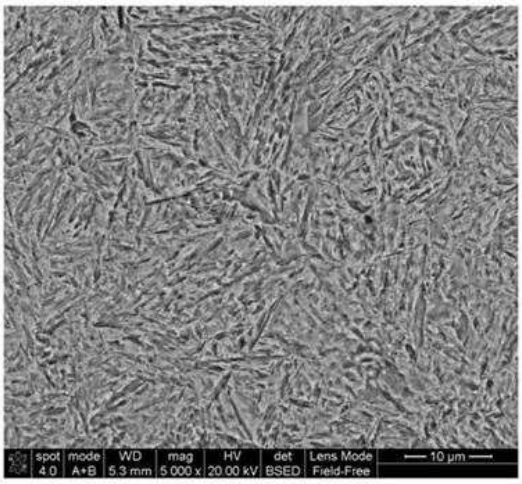

Fig. 3 Microstructure of oil-quenched block sample.

The retained austenite was detected using XRD analysis, Figure 1. Quantitative results of the XRD analysis are listed in Table 2, including the volume fractions and carbon contents of retained austenite, lath-type martensite (M_{II}) and plate-type martensite (M_I), the broadening (full-width-at-half-maximum)

Table 2 Quantitative results of XRD measurements of all the tested samples.

Sample	HV	Retained austenite		Peak broadening		M_I		M_{II}		M
		Vol.%	C%	$\{200\}_M$	$\{211\}_M$	Vol.%	C%	Vol.%	C%	C%
1	742±9	8.0±0.6	0.90	1.39	1.32	57.3	0.41	34.7	0.19	0.32
2	677±17	8.4±1.8	0.90	1.22	1.19	46.2	0.40	45.4	0.18	0.29
3	588±14	-	-	1.02	0.96	47.7	0.37	52.3	0.05	0.20
4	542±4	-	-	0.87	0.83	55.9	0.25	44.1	0.06	0.17
5	717±3	3.4±0.1	1.02	1.16	1.09	44.7	0.55	51.8	0.10	0.33
6	704±11	1.9±0.4	1.04	0.99	1.02	52.5	0.41	45.5	0.15	0.29
7	464±13	3.6±0.6	1.18	0.73	0.73	40.8	0.33	55.3	0.01	0.15
8	422±16	3.9±1.7	1.28	0.56	0.56	46.7	0.17	49.0	0	0.08

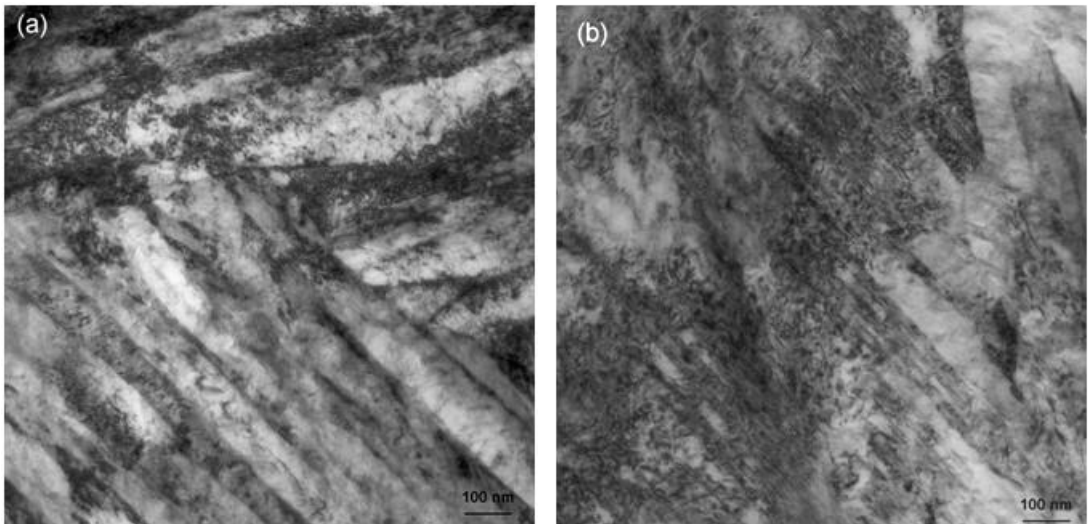

Fig. 4 TEM bright field images of (a) lath-type martensite and (b) plate-type martensite.

of the martensite diffractions $\{200\}_M$ and $\{211\}_M$, and the overall carbon content of martensite. The as-quenched steel contains approximately 8.0% retained austenite and the carbon content of the austenite is approximately 0.90%. The tetragonal ratios of lath- and plate-type martensites were determined to be 1.0146 and 1.0066 respectively, which correspond to the carbon content of 0.19 for the martensite laths and 0.41 for the martensite plates. The volume fraction of the lath- and plate-like martensites was estimated, according to the intensities of the separated sub-peaks, to be 34.7% and 57.3% respectively. The co-existence of lath- and plate-like martensites has been verified in TEM observation, as shown in Figure 4. In Figure 4a, the martensite exhibits parallel laths in each block grain, in which the sub-structure is dislocations. In Figure 4b, a martensite place shows high density of twins.

So far, two types of martensitic structures of different carbon contents and sub-structures have been transformed from under-cooled austenite in the continuous oil-quench. The results reveal that carbon partitioning can take place not only in isothermal transformations as reported in the literature [3, 7, 14-18], but also in continuous cooling. Unlike the qualitative prediction or description in earlier studies[10-13], precise quantitative analysis of the carbon partitioning has become realistic in the presented work.

For the kinetics of carbon partitioning, because the Ms temperature of the investigated medium carbon alloyed steel is higher than 200^0C, effective diffusion of carbon atoms from the supersaturated martensitic lattice to the adjacent austenite was feasible especially in the early stage of the transformation, leading to the formation of lath-type martensites. Consequently the remaining austenite became enriched in carbon, which transformed to plate-type martensites when the temperature was progressively lower. When the transformation was terminated at room temperature, carbon enrichment resulted in the retained austenite.

2.2 Effect of cooling rate on carbon partitioning

Samples 5-8 in Tables 1 and 2 illustrate the effect of cooling conditions on the microstructure and carbon partitioning behaviour. In these samples, air-cooling provided a slower cooling rate than oil-quench, whereas in both cases the core regions should have cooled more slowly than the surface edges.

Typical microstructures of the two samples are shown in Figure 5. The oil-quenched sample shows predominantly laths and plates of martensite, whereas the air-cooled sample was only partially transformed to martensite for the presence of carbide precipitates in some region. Such regions were easily recognized in the metallographic sample preparation because the ferrite-carbide mixture showed faster etching than the martensite and retained austenite regions.

The hardness measurements reveal a decrease of hardness with decreasing cooling rate, e.g. from HV717 at the oil-quenched sample edge to HV422 at the air-cooled central region. The decrease of hardness is directly related to the reduced straining of the martensite or ferrite matrix, seeing the measured peak broadening of the martensite or ferrite diffractions $\{200\}_M$ and $\{211\}_M$ in Table 2.

The XRD analyses performed on the four regions (Samples 5-8 in Table 2) reveal the behaviour of carbon partitioning dependent on the cooling rate. In the first, although all the samples show small volume

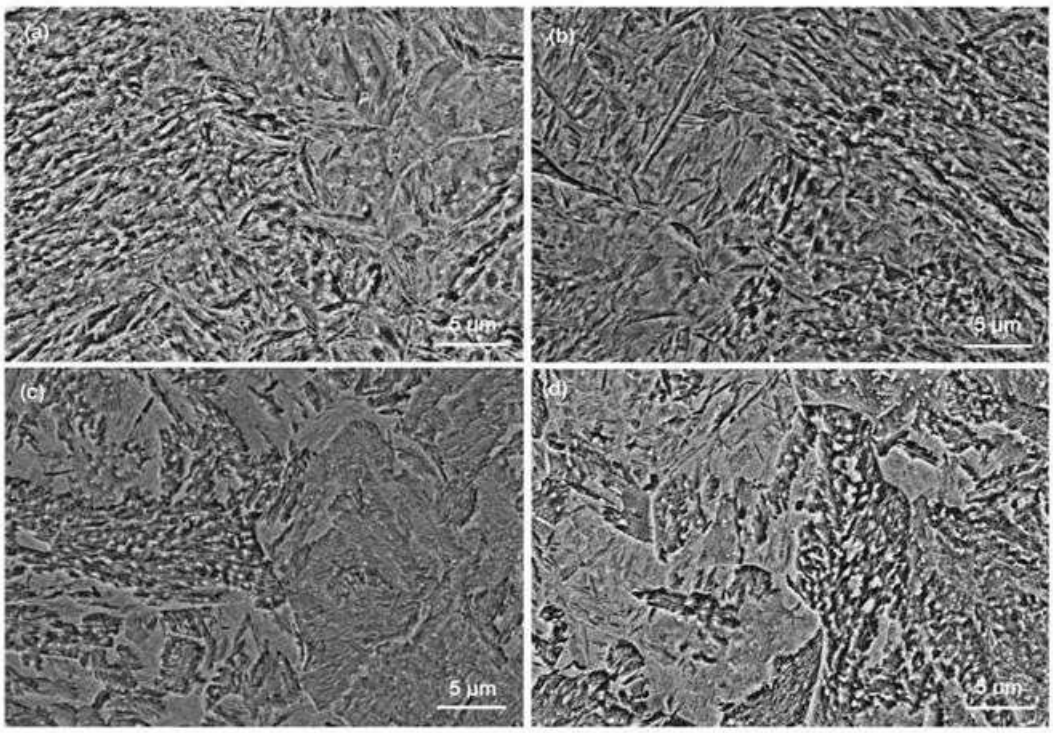

Fig. 5 SEM images of an oil-quenched thick rod of 50 mm in diameter: (a) at depth of 5 mm; (b) at the core; (c) and (d) air-cooled surface and core areas.

fractions of retained austenite, the austenite carbon contents are remarkably higher than the nominal carbon content of the sample and more importantly, increase with decreasing cooling rate. In other words, slower cooling led to enhanced carbon enrichment in the retained austenite. Secondly, the XRD results show a decrease of carbon contents in the martensites, i.e. from 0.55% at the edge of the oil-quenched sample to 0.18% at the core of the air-cooled sample for M_I. In particular, the M_{II} sub-phase in the air-cooled sample shows extremely low carbon contents, which is consistent to the carbide precipitation. The overall carbon content of the martensite has decreased from 0.33% of the oil-quenched sample edge to 0.09% of the air-cooled sample core region.

2.3 Microstructure and carbon partitioning in tempering samples

Figure 6 shows high magnification SEM images of the three tempered samples (Samples 2-4 in Table 1). Whereas the three samples still retained the as-quenched martensitic morphology, carbide precipitates observed in both the 300^0C and 400^0C tempered samples evidenced the structural evolution. The structural evolution was accompanied by the softening of the steel from HV742 to HV542, Table 1.

The 200^0C tempered sample showed little change in the retained austenite, but remarkable recovery of lattice strains in the tempered martensite. The overall carbon content of martensite has been decreased from 0.32% to 0.29%. Then with increasing tempering temperature from 200^0C to 400^0C, further pronounced recovery of the martensite strains took place along with the decrease of carbon contents in both the lath-type martensite (M_{II}) and plate-type martensite (M_I). The variation of the martensite carbon contents can be explained by the homogeneous precipitation of carbides in the martensite matrix, Figure 6 b-c.

3. Conclusions

(1) Using a sample material of alloyed medium carbon steel, a series of continuous hardening treatments have been carried out followed by a number of tempering treatments at selected temperatures from 200^0C to 400^0C. A self-developed multiple Gaussian peak-fitting technique has been introduced to perform quantitative analysis of the carbon contents of the resulting martensite and austenite constituents.

(2) Significant carbon partitioning has been found to take place during the phase transformation from under-cooled austenite to martensite, resulting in different carbon contents between the retained austenite and the martensite. In particular, two types of martensite constituents having different carbon

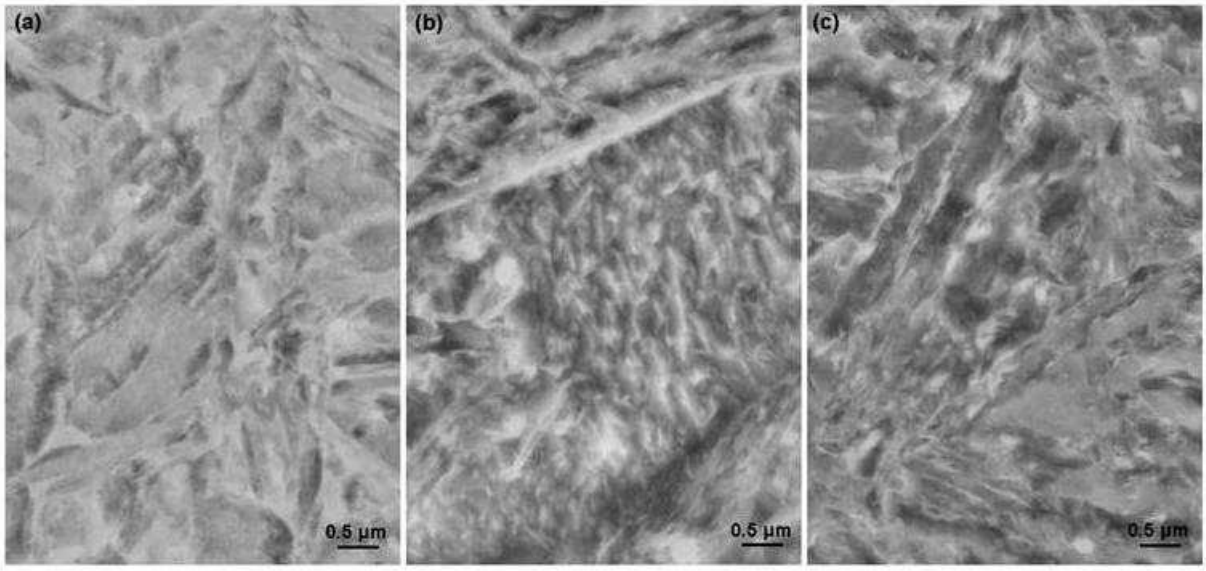

Fig. 6 SEM images of oil-quenched block samples after tempering at various temperatures: (a) tempered at 200^0C; (b) tempered at 300^0C and (c) tempered at 400^0C.

contents have been determined by using the combined FEG-SEM, XRD and TEM analyses.

(3) Slower cooling rates in thick samples have been found to facilitate more pronounced carbon partitioning, which included the diffusion of carbon from the newly formed martensite to the un-transformed austenite and the precipitation of carbide particles in the martensite/ferrite matrix.

(4) Subsequent tempering, following the quenching treatment, resulted in the recovery of lattice strains in the martensite and, when tempered at 300^0C or higher temperatures, significant decrease of the carbon contents within the martensite.

Acknowledgment

Partial financial support from UK government through a Technology Strategy Broad project (Smart Grant No.720113) is acknowledged. The authors thank Dr. Shuncai Wang, in University of Southampton, for providing the electrochemical polishing in TEM sample preparation.

References

1 Caballero FG, Bhadeshia HKDH, Mawell KJA, Jones DG, Brown P, Design of novel high strength bainitic steels[J], Mater Sci Technol, 2001, 17: 512-522.

2 Caballero FG, Bhadeshia HKDH, Very strong bainite[J], Curr Opin Solid State Mater, 2004, 8: 251-257.

3 Bhadeshia HKDH, Review: Nanostructured bainite[J], Proc R Soc, 2010, A466: 3-18.

4 Wang TS, Li XY, Zhang FC, Zheng YZ, Microstructures and mechanical properties of 60Si2CrVA steel by isothermal transformation at low temperature[J], Mater Sci Eng, 2006, A438-440: 1124-1127.

5 Yang J, Wang TS, Zhang B, Study on bainitic microstructure under low austempering temperature and its wear resistance of high carbon low alloy steel[J], J Yanshan University, 2011, 35: 427-451.

6 Edmonds DV, He K, Rizzo FC, De Cooman BC, Matlock DK, Speer JG, Quenching and partitioning martensite – A novel steel heat treatment[J], Mater Sci Eng, 2006, A438-440: 25-34.

7 Clarke AJ, Speer JG, Miller MK, Hackenberg RE, Edmonds DV, Matlock DK, Rizzo FC, Clarke KD, De Moore S, Carbon partitioning to austenite from martensite or bainite during the quench and partition (Q&P) process: A critical assessment[J], Acta Mater, 2008, 56: 16-22.

8 Zhang K, Zhang M, Guo Z, Chen N, Rong Y, A new effect of retained austenite on ductility enhancement in high-strength quenching-partitioning-tempering martensitic steel[J], Mater Sci Eng, 2011, A528: 8486-8491..

9 Rong Y, Advanced Q-P-T steels with ultrahigh strength-high ductility[J], Acta Metall Sinica, 2011, 47: 1483-1489.

10 Matas S, Hehemann RF, Retained austenite and the tempering of martensite[J], Nature, 1960, 187:685-686.

11 Hsu TY, Li XM, Diffusion of carbon during the formation of low-carbon marteniste[J], Script Metall, 1983, 17: 1285-1288.

12 Bhadeshia HKDH, Carbon content of retained austenite in quenched steels[J], Met Sci, 1983, 17: 151-152.

13 Mujahid SA, Bhadeshia HKDH, Partitioning of carbon from supersaturated ferrite plates[J], Acta Metall Mater, 1992, 40: 389-396.

14 Speer JG, Edmonds DV, Rizzo FC, Matlock DK, Partitioning of carbon from supersaturated plates of ferrite, with application to steel processing and fundamentals of the bainite transformation[J], Curr Opin Solid State Mater, 2004, 8: 219-237.

15 Chupatanakul S, Nash P, Dilatometric measurement of carbon enrichment in austenite during bainite transformation[J], J Mater Sci Lett, 2006, 41: 4965-4969.

16 Garcia-Mateo C, Caballero FG, Miller MK, Jimenez JA, On measurement of carbon content in retained austenite in a nanostructured bainitic steel[J], J Mater Sci, 2012, 57: 1004-1010.

17 Speer J, Matlock DK, De Cooman BC, Schroth JG, Carbon partitioning into austenite after martensite transformation[J], Acta Mater, 2003, 51: 2611-2622.

18 Ooi SW, Cho YR, Oh JK, Bhadeshia HKDH, Carbon enrichment in residual austenite during martensitic transformation[C], in ICOMAT-08, edit. G.B. Olson, D.S. Lieberman, A. Saxena, The Mineral, Metals and Materials Society, 2009, 179-185.

19 Caballero FG, Miller MK, Clarke AJ, Garcia-Mateo C, Examination of carbon partitioning into austenite during tempering of bainite[J], Script Mater, 2010, 63: 442-445.

20 Abbaschian R, Abbeschian L, Reed-Hill RE, Physical Metallurgy Principles[M], 4th Edition. 1994, Cengage Learning, Stanford, USA, p623-624.

21 Garg A, McNelley TR, Estimation of martensite carbon content in as-quenched AISI 52100 steel by X-ray diffraction[J], Mater Lett, 1986, 4: 214-218.

22 Lawrynowicz Z, Carbon partitioning during bainite transformation in low alloy steels[J], Mater Sci Technol, 2002, 18: 1322-1324.

23 Luo Q, Wang C, Zhou Z, Chen L, Structure characterization and tribological study of magnetron sputtered nanocomposite nc-TiAlV(N, C)/a-C coatings[J], J Mater Chem, 2011, 21 (26): 9746 - 9756.

24 Luo Q, Zhou Z, Rainforth WM, Hovsepian PE, TEM-EELS study of low-friction super-lattice TiAlN/VN coating: The wear mechanisms [J], Tribo Lett, 2006, 24: 171-178.

25 Pardal JM, Tavares SSM, Fonseca MPC, Abreu HFG, Silva JJM, Study of austenite quantification by XRD in the 18Ni-Co-Mo-Ti maraging 300 steel[J], J Mater Sci, 2006, 41: 2301-2307.

26 Luo Q, Chi K, Li S, Barnard P, Microstructural Stability and Lattice Misfit Characterisations of Nimonic 263[C], Proceedings of the ASME 2012 Pressure Vessels & Piping Division Conference (PVP2012), July 15-19, 2012, Toronto, Ontario, Canada.

27 Luo Q, Jones AH, High-precision determination of residual stress of polycrystalline coatings using optimised XRD-sin2ψ technique[J], Surf Coat Technol, 2010, 205: 1403-1408.

28 Krauss G, Deformation and fracture in martenitic carbon steels tempered at low temperatures[J], Metall Mater Trans, 2001, 32B: 205-221.

Corresponding author: Dr. Quanshun Luo
Email: q.luo@shu.ac.uk
Mail address: Materials and Engineering Research Institute, Sheffield Hallam University, Howard Street, Sheffield, S1 1WB, United Kingdom.
Tel : 0044 114 2253649
Fax: 0044 114 2253501.